energies

MDPI

Article

Experimental Evaluation of Enhanced Oil Recovery in Shale Reservoirs Using Different Media

Jiaping Tao [1,2], Siwei Meng [1,2,*], Dongxu Li [3], Lihao Liang [1] and He Liu [1,2]

[1] PetroChina Research Institute of Petroleum Exploration & Development, Beijing 100083, China; taojiaping93@sina.com (J.T.)
[2] State Key Laboratory of Continental Shale Oil, Daqing 163002, China
[3] PetroChina Daqing Oilfield Co., Ltd., Daqing 163002, China
* Correspondence: mengsw@petrochina.com.cn

Abstract: The presence of highly developed micro-nano pores and poor pore connectivity constrains the development of shale oil. Given the rapid decline in oil production , enhanced oil recovery (EOR) technologies are necessary for shale oil development. The shale oil reservoirs in China are mainly continental and characterized by high heterogeneity, low overall maturity, and inferior crude oil quality. Therefore, it is more challenging to achieve a desirably high recovery factor. The Qingshankou Formation is a typical continental shale oil reservoir, with high clay content and well-developed bedding. This paper introduced high-precision non-destructive nuclear magnetic resonance technology to carry out a systematic and targeted study. The EOR performances and oil recovery factors related to different pore sizes were quantified to identify the most suitable method. The results show that surfactant, CH_4, and CO_2 can recover oil effectively in the first cycle. As the huff-and-puff process continues, the oil saturated in the shale gradually decreases, and the EOR performance of the surfactant and CH_4 is considerably degraded. Meanwhile, CO_2 can efficiently recover oil in small pores (<50 nm) and maintain good EOR performance in the second and third cycles. After four huff-and-puff cycles, the average oil recovery of CO_2 is 38.22%, which is much higher than that of surfactant (29.82%) and CH_4 (19.36%). CO_2 is the most applicable medium of the three to enhance shale oil recovery in the Qingshankou Formation. Additionally, the injection pressure of surfactant increased the fastest in the injection process, showing a low flowability in nano-pores. Thus, in the actual shale oil formations, the swept volume of surfactant will be suppressed, and the actual EOR performance of the surfactant may be limited. The findings of this paper can provide theoretical support for the efficient development of continental shale oil reservoirs.

Keywords: high clay content; huff-and-puff; nuclear magnetic resonance; T_2 spectrum; quantitative evaluation

Citation: Tao, J.; Meng, S.; Li, D.; Liang, L.; Liu, H. Experimental Evaluation of Enhanced Oil Recovery in Shale Reservoirs Using Different Media. *Energies* **2024**, *17*, 3410. https://doi.org/10.3390/en17143410

Academic Editor: Reza Rezaee

Received: 10 June 2024
Revised: 4 July 2024
Accepted: 5 July 2024
Published: 11 July 2024

1. Introduction

Unconventional oil and gas resources are playing an increasingly significant role in the development of the oil and gas industry, with their abundant reserves and great exploration and development potential. Shale oil is considered the most valuable unconventional oil and gas resource for development [1–3]. The shale oil revolution in the US has rapidly increased oil production in America and profoundly changes the global energy landscape. China has rich deposits of shale oil; the geological reserves of shale oil in China are about 28.3 billion tons, showing great potential for development [4–6]. The scaled-up cost-effective recovery of shale oil is of critical strategic value for the sustained development of China's petroleum industry.

Shale oil reservoirs possess highly developed micro-nano pores, with poor pore connectivity and extremely low permeability [7–9]. They require the use of horizontal wells and multi-stage fracturing technologies to achieve beneficial development [10–12]. However,

the production of shale oil wells suffers from rapid production decline. The production of a fractured shale oil well in the US declines by about 70% after one year of production, and the recovery factor is typically less than 10% [13,14]. Compared with the largely marine shale oil reservoirs of the US, shale oil reservoirs in China are generally formed in continental sedimentary environments. They are characterized by small distribution area, high heterogeneity, low overall maturity, and inferior crude oil quality, and therefore, it is challenging to achieve a desirably high recovery factor [15–18]. Given the above-stated obstacles, enhanced oil recovery (EOR) treatments are necessary for improving shale oil recovery and mitigating well production decline.

The ultra-low porosity and permeability of shale oil reservoirs severely reduce the applicability of conventional EOR technologies to effectively enhance shale oil recovery. Therefore, strengthening the research and development of shale-appropriate EOR technologies is an important direction for future development. Previous research demonstrates that the gas huff-and-puff process and surfactant imbibition are currently more feasible technologies for the EOR of shale oil [19–23]. With the appropriate schemes of post-frac well soaking and production, the gas huff-and-puff method can efficiently supplement energy formation and enhance oil recovery [24,25]. Through the mechanisms of wettability alteration and interfacial tension reduction, surfactant imbibition can also effectively enhance oil recovery [26,27].

The Songliao Basin is a typical large continental sedimentary basin, possessing abundant hydrocarbon resources. The Qingshankou and Nenjiang Formations, which were formed in the Late Cretaceous period, are the main source rocks for the basin, with their high-quality organic-matter-rich shale [28,29]. Preliminary exploration shows that the shale oil geological reserves of the Qingshankou Formation reach about 5.46 billion tons, and it is this gargantuan development potential that makes this layer the main field for shale oil development in the Daqing Oil Field. In recent years, breakthroughs have been made in the production practices of Qingshankou shale oil. In order to support exploration and development, researchers have carried out a large number of basic studies on the Qingshankou Formation. Liu et al. clarified the shale oil exploration "sweet spots", based on the detailed description and analysis of the cores and shale lithofacies characteristics [30]. Yuan et al. proposed the key theoretical and technical issues and countermeasures for effective development, targeting reservoir characteristics [31]. Yang et al. employed nanoscratch technology to continuously investigate the damage and failure mechanisms of the Qingshankou Formation, which is one of the most important measurement methods for studying water–CO_2–shale interaction [32,33].

Related studies have stimulated the development of Qingshankou shale oil. However, due to the high clay content and well-developed bedding of the Qingshankou Formation [30,34,35], the shale oil wells still suffer from the rapid production decline in the production stage. In this situation, the recovery of shale oil is very low, and it is difficult to achieve beneficial development. Therefore, targeted EOR studies are urgently needed to identify the most suitable EOR technology for recovering Qingshankou shale oil. Targeting the characteristics of the Qingshankou Formation, this paper introduced high-precision non-destructive nuclear magnetic resonance (NMR) technology to carry out a systematic study. Multicycle huff-and-puff experiments using surfactant, CH_4, and CO_2 were performed under the reservoir conditions using cores and crude oil collected from the Qingshankou Formation. The oil recovery factor for different pore sizes was quantified during the multicycle huff-and-puff process; the EOR performances of different EOR technologies in the Qingshankou Formation were compared to identify the most suitable method. The findings of this paper can provide theoretical support for the efficient development of the Qingshankou Formation shale oil.

2. Experimental Section

2.1. Sample Preparation

The shale samples used in this paper were collected from the Qingshankou Formation in the Songliao Basin. The Qingshankou Formation is mostly shale, with local interbeds of sandstone, limestone, and limy mudstone. The shale, predominantly composed of clay minerals, quartz, feldspar, and carbonates, possesses well-developed nano pores and micro fractures. The crude oil used in this paper was collected from the production well. According to the slim-tube test, the minimum miscibility pressure between CO_2 and crude oil was 23.9 MPa. The viscosity of this oil is 1.51 mPa·s at 90 °C.

Collected core samples were formed into cylindrical specimens (5 cm × Φ2.5 cm) via wire-cutter machining. Then, the specimens with an intact appearance and no considerable fracture were selected and polished using abrasive paper to obtain a smooth surface and flattened ends. Finally, the polished specimens were treated with petroleum ether and benzene to remove crude oil in these cores. The specimens were inspected to ensure that they were intact and undamaged during oil removal.

2.2. Experimental Apparatus and Methods

The AP-608 Automated Permeameter-Porosimeter (Figure 1), from Coretest systems, was used to measure the porosity and permeability of the Qingshankou Formation shale. The available confining pressure of the apparatus is 0–9000 psi, and the measurement ranges of porosity and permeability are 0.1–40.0% and 0.001 mD–10,000 mD, respectively. During the experiments, the oil-removed shale specimens were dried at 60 °C in the oven for 24 h before being placed in the core holder. The confining pressure was set at 3000 psi for the porosity and permeability measurements. The measured initial porosity and permeability of the selected shale specimens are listed in Table 1.

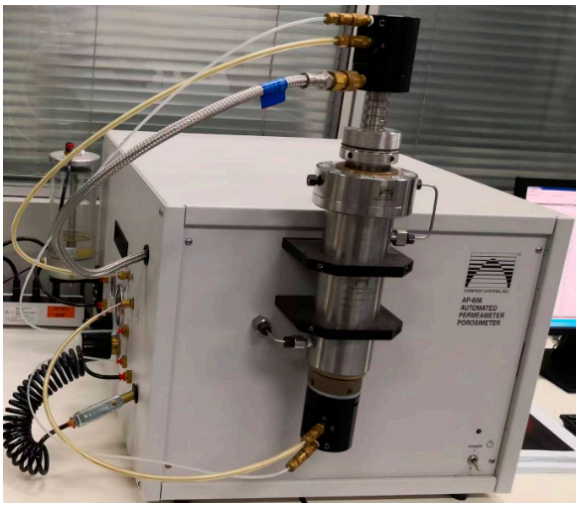

Figure 1. Experimental equipment used for porosity and permeability analysis.

Table 1. Core parameters of shale samples.

Sample	Diameter (cm)	Length (cm)	Porosity (%)	Permeability (mD)
1	2.50	5.00	5.31	0.0254
2	2.49	5.01	4.58	0.0428

Multicycle huff-and-puff physical simulation experiments: The schematic depiction of the experimental apparatus is shown in Figure 2. The apparatus mainly consists of an ISCO pump, an intermediate container, a core holder, a hand pump, and two pressure gauges. In these experiments, the following assumptions were adopted: the samples can represent the geological characteristics of the target formation, and the damage to the specimens during

processing can be ignored. After saturation, the oil distribution in the cores can represent the actual occurrence of crude oil in the formation. The physical simulation experiment meets the requirements of the main influencing factors, based on the similarity criteria. The experimental procedures are briefly described as follows. (1) Use the wire cutter to cut the specimen in half radially. (2) Place the specimen in the intermediate container and hold under vacuum for 24 h. Then, saturate the specimen with crude oil, and record the volume of oil saturated into the specimen. (3) Place the specimen in the NMR apparatus to obtain the T_2 spectrum distribution to analyze the oil distribution under the saturated state. (4) Place the specimen in the core holder and constantly maintain the confining pressure at 2 MPa higher than the injection pressure. Continuously inject surfactant/CH_4/CO_2 into the specimen until the injection pressure reaches 30 MPa. Then, close the inlet valve and soak the specimen for 24 h. (5) After soaking, open the inlet valve and record the oil production. Then, obtain the T_2 spectrum distribution using the NMR apparatus to analyze the oil distribution after the huff-and-puff process. (6) Repeat Steps (4) and (5) to perform four huff-and-puff cycles to analyze the EOR performance of surfactant/CH_4/CO_2 in the shale cores. The surfactant used in this experiment is a kind of petroleum sulfonate, with a concentration of 0.3 wt%. According to the conditions of the Qingshankou Formation, the pressure and temperature during these experiments were set at 30 MPa and 90 °C, respectively.

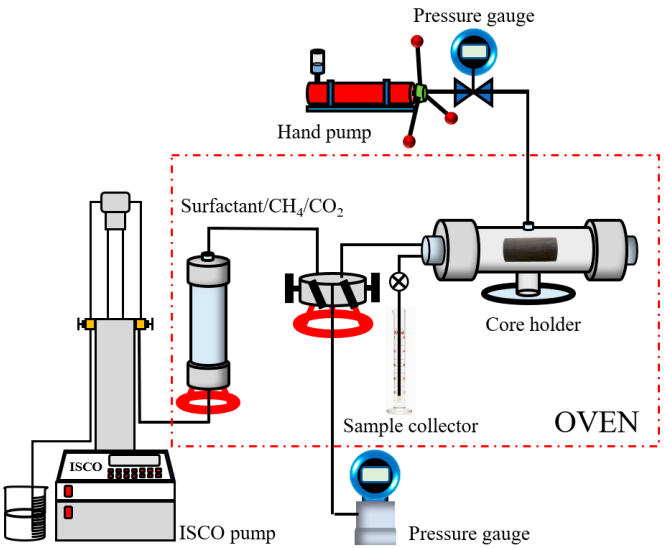

Figure 2. Schematic depiction of the experimental setup for huff-and-puff.

3. Results and Discussion

3.1. Analysis of EOR Performance of Surfactant in Shale Oil Reservoirs

Surfactant was continuously injected into the shale core until the injection pressure reached 30 MPa. Then, the core holder was sealed for 24 h, after which the inlet valve was opened for oil production. The experimental temperature was kept at 90 °C throughout the experiment. The T_2 spectrum was measured after each cycle of surfactant huff-and-puff to analyze the oil distribution in pores of different sizes in the shale cores.

The photos of Specimen 1-1 at different stages of the huff-and-puff process are shown in Figure 3. The surface of the oil-saturated shale core is dark black, with notable oil traces. With the progress of the surfactant huff-and-puff process, the core surface becomes drier. After three cycles of huff-and-puff, there were no notable oil traces on the core surface. The color of the shale core is also fading during the experiment. The change in the shale core is attributed to the oil production from the shale, and the mentioned phenomenon is significant, as noted in the comparison between the core photos at 0 H and 96 H. It is demonstrated that surfactant can diffuse into the micro pores of shale during soaking, helping to produce oil in such pores. This finding is also supported by the T_2 spectrums.

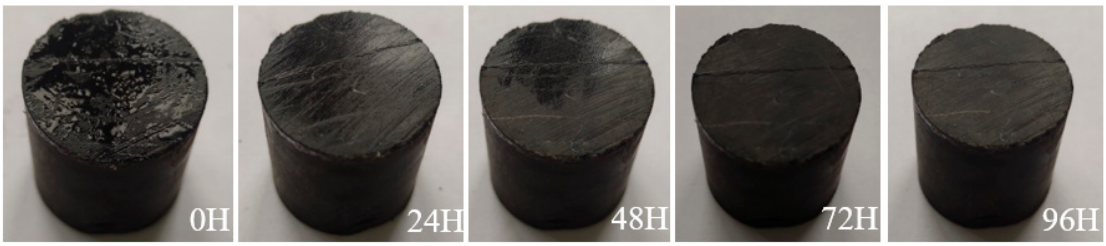

Figure 3. Shale core sample after surfactant huff-and-puff.

The T_2 spectrums of Specimen 1-1 at different stages of the huff-and-puff process are shown in Figure 4. The T_2 spectrum of oil-saturated Specimen 1-1 has two peaks, with the left peak being higher than the right one. This indicates that the nano-scale pores are well developed in the shale. The radii of the pores are predominantly smaller than 50 nm, and larger pores are relatively limited.

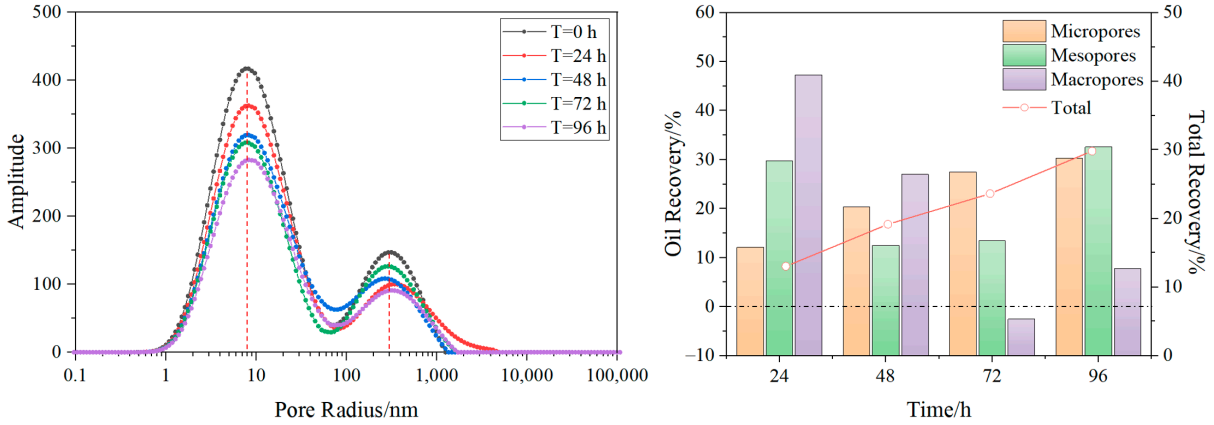

Figure 4. T_2 spectrums and oil recovery after surfactant huff-and-puff.

During the surfactant huff-and-puff experiment, the oil in the core is effectively recovered. After the first cycle of huff-and-puff, the oil recovery factor reaches 13.03%. The amount of oil produced in the small pores is significant—the amount of oil produced in pores with radii smaller than 50 nm (the small scale) is 12.12%; for those 50–500 nm (the medium scale), it is 29.76%; for those larger than 500 nm (the large scale), it is 47.31%. The oil recovery of the second cycle is 19.14%. Specifically, the amount of oil produced in the small pores is 20.36%, with a significant increase. However, as a part of the oil migrates from smaller pores to larger ones, the oil in the larger pores increases, and the amount of oil produced in medium (50–500 nm) and large (>500 nm) pores drop to 12.48% and 26.97%; both values are lower than those of the first cycle. The recovery factor grows to 23.62% and 29.82% after the third and fourth cycles, respectively. The amount of oil produced in the small pores continues to increase to 27.45% and 30.30%, respectively. That of the medium pores grows to 13.50% and 32.56% in the third and fourth cycles, while that of the large pores falls to −2.53% and 7.76%, respectively, due to the migration of the oil in the small and medium pores to the large pores.

The above results show that the surfactant exhibits good EOR performance for the Qingshankou Formation shale. During the surfactant huff-and-puff process, the oil in the small pores (with radii below 50 nm) of the shale is gradually recovered, with the corresponding amounts produced climbing constantly. For medium and large pores (with radii of 50–500 nm and >500 nm, respectively), the produced amounts are generally positive. Occasionally, there is a phenomenon of an increase in oil occurrence in larger pores, as a part of the oil in the small pores and throats migrates to the larger pores during the huff-and-puff process.

3.2. Analysis of EOR Performance of CH_4 in Shale Oil Reservoirs

Similarly, CH_4 was continuously injected into the shale core until the pressure reached 30 MPa, and flowback and production were executed after 24 h of soaking. The experimental temperature throughout the experiment was also 90 °C. The oil distribution at different stages of CH_4 huff-and-puff was captured using NMR to reveal the EOR performance of CH_4 in the shale oil reservoirs.

The photos of Specimen 2-1 at different stages of the huff-and-puff process are shown in Figure 5. The surface of Specimen 2-1 is dark black, with notable oil traces. As huff-and-puff proceeds, the specimen becomes drier, and the oil traces fade away. The color of the shale core also changes; it gradually becomes lighter in some zones. The stated phenomenon is significant when compared to that noted in the photos at 0 H and 96 H. It can be concluded that the injected CH_4 effectively recovered oil in the pores of the shale during soaking.

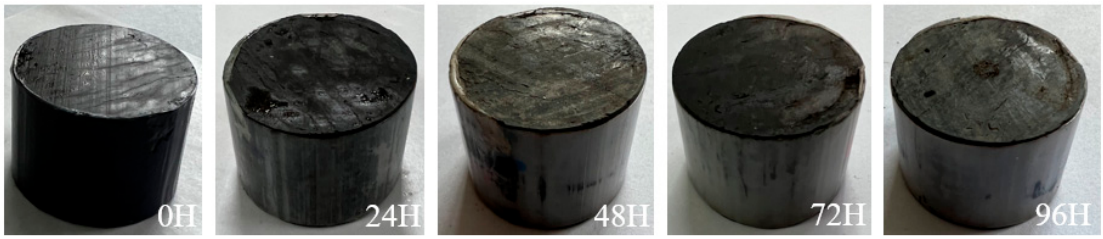

Figure 5. Shale core sample after CH_4 huff-and-puff.

The T_2 spectrums of Specimen 2-1 at different stages of CH_4 huff-and-puff are shown in Figure 6. After oil-saturation, the T_2 spectrum of the shale core exhibits three peaks, a high peak on the left, and two small peaks in the middle and right, which demonstrates the significant development of nano-scale pores in shale, with the majority of pores smaller than 50 nm. For such shale, there are fewer larger pores, and it is difficult to recover the oil.

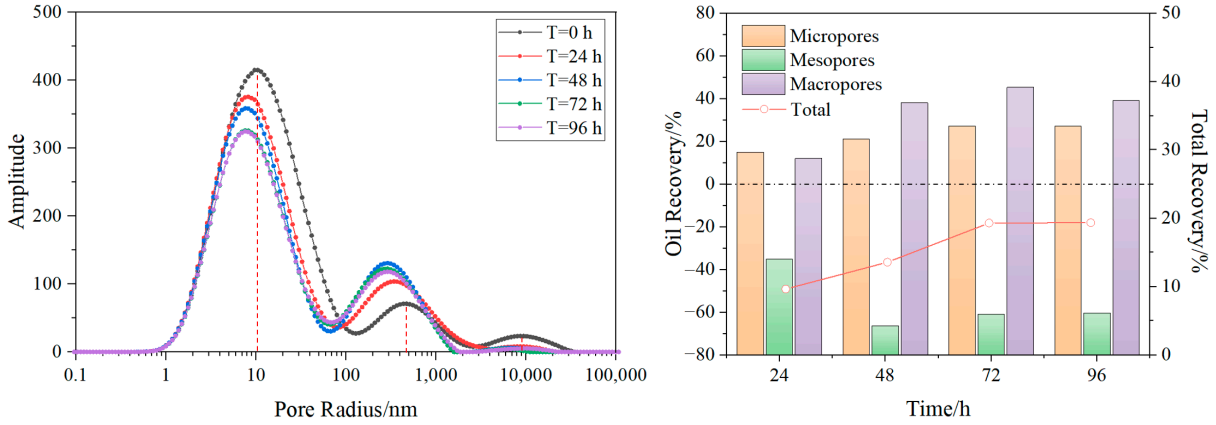

Figure 6. T_2 spectrums and oil recovery after CH_4 huff-and-puff.

The EOR effect of the CH_4 huff-and-puff process is relatively poor in the shale core. The oil recovery is 9.65% after the first cycle of huff-and-puff, and the oil in the small pores (<50 nm) is effectively produced (at 14.90%). Due to the migration of oil from the smaller pores to the larger pores, the oil content in the medium pores (50–500 nm) grows, and the production rate is −35.15%. The amount of oil produced in the large pores (>500 nm) is 12.1%. After the second and third cycles, the oil recovery rates are 13.58% and 19.30%, respectively. The oil production rate of the small pores (<50 nm) rises to 21.04% and 27.24%, respectively. As a large quantity of oil transfers from the small to medium (50–500 nm) pores, the oil in the latter increases considerably, and the production levels drop to −66.39% and −60.83%, respectively. In these two cycles, the oil in the large pores (>500 nm) is

effectively recovered (at 38.11% and 45.23%). However, the EOR performance of CH_4 is degraded rapidly in the fourth cycle. The oil recovery factor after the fourth cycle is only 19.36%, nearly equal to that after the 3rd cycle. The oil production rates exhibit no notable changes, regardless of pore sizes.

3.3. Analysis of EOR Performance of CO_2 in Shale Oil Reservoirs

Similarly, the CO_2 multicycle huff-and-puff physical simulation experiments were performed at 90 °C and 30 MPa. During the four cycles of CO_2 huff-and-puff, the differentiation of oil production from different-sized pores was clarified via the T_2 spectrums, and the EOR performance of CO_2 in the shale oil reservoirs was assessed.

The photos of Specimen 1-2 and 2-2 at different stages of CO_2 huff-and-puff are shown in Figures 7 and 8. The cores are also dark black, with notable oil traces on their surface after oil saturation. With the ongoing CO_2 huff-and-puff process, the oil inside the cores is recovered, and the surface oil traces are reduced. The color of these cores gradually fades, and some zones even change from black to light grey. The above results demonstrate the high EOR capacity of CO_2 in shale, as CO_2 can diffuse into the tiny pores of the shale and help to effectively recover oil in such pores.

Figure 7. Shale core sample 1-2 after CO_2 huff-and-puff.

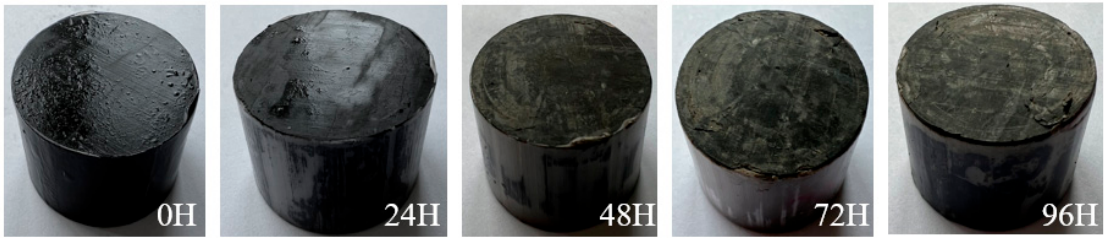

Figure 8. Shale core sample 2-2 after CO_2 huff-and-puff.

The T_2 spectrums of Specimen 1-2 at different stages of CO_2 huff-and-puff are shown in Figure 9. The T_2 spectrum of Specimen 1-2 is bimodal after oil saturation. A high left peak associated with a low right peak shows that the shale possesses highly developed nano-scale pores. The majority of pores have radii smaller than 50 nm, and the quantity of larger pores is limited. It is difficult to recover oil from such shale.

During CO_2 huff-and-puff, oil is effectively produced in the shale core. After the first cycle of CO_2 huff-and-puff, the oil recovery reaches 8.98%. Moreover, the oil in the small pores (<50 nm) is efficiently recovered at a rate of 11.99%. The amount of oil produced in the medium pores (50–500 nm) reaches 4.69%, and for large pores (>500 nm), it is −35.71%, due to oil migration from the smaller to the larger pores. The second cycle also effectively recovers oil from the shale. The oil recovery increases to 18.02%, and the amount of oil produced in the small pores rises considerably (to 20.43%). The amount of oil produced in the medium pores (50–500 nm) is 16.69%, and for the large pores (>500 nm), it is −30.29%. CO_2 maintains excellent EOR performance in the third cycle, i.e., the oil recovery rate rises to 30.98%, which is much higher than that after three cycles of surfactant huff-and-puff. The amount of oil produced in the small (<50 nm) and medium (50–500 nm) pores continue to grow (25.84% and 64.77%, respectively). As oil flows from the small and medium pores

to the large pores, the oil produced by the latter (>500 nm) falls to −52.05%. In the fourth cycle, the EOR performance of CO_2 is slightly degraded. The recovery factor grows to 34.04%, and is associated with small incremental increases in the amount of oil produced by the small and medium pores (28.13% and 65.79%, respectively). Nevertheless, the oil in the large pores (>500 nm) is effectively recovered during this period, and the production rate increases from −52.05% to −18.66% (this negative value means that the amount of oil in the large pores after the fourth cycle is still greater than the initial amount observed in the large pores). During the CO_2 huff-and-puff, the oil recovery factor is 4.22% higher than that noted for the surfactant huff-and-puff process.

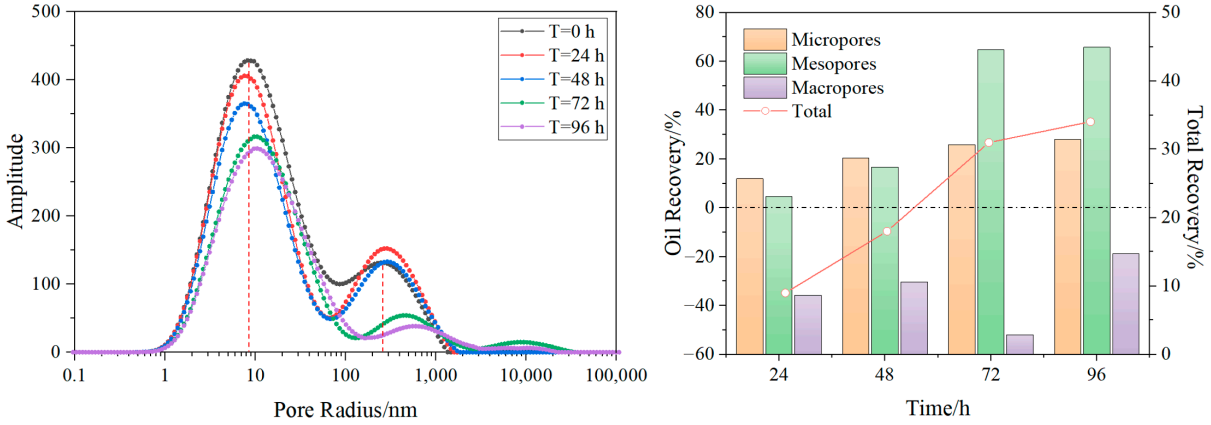

Figure 9. T_2 spectrums and oil recovery of core 1-2 after CO_2 huff-and-puff.

The T_2 spectrums of Specimen 2-2 after different stages of CO_2 huff-and-puff are shown in Figure 10. The T_2 spectrum of the oil-saturated core exhibits three peaks, with the higher left peak and lower middle and right peaks indicating the significant development of nano-scale pores in the shale. The oil is mostly stored in pores with radii smaller than 50 nm, which leads to high difficulties in oil recovery.

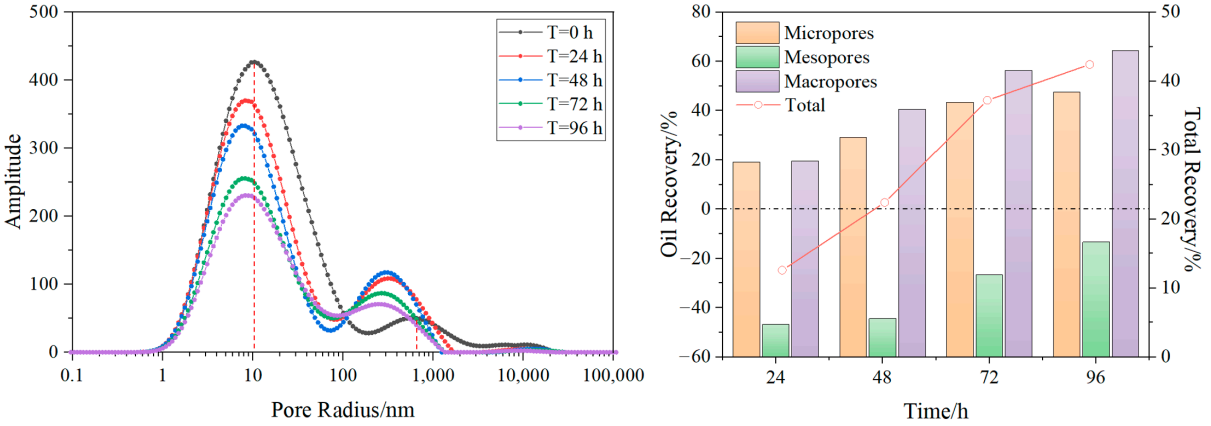

Figure 10. T_2 spectrums and oil recovery of core 2-2 after CO_2 huff-and-puff.

Similar to the case of Specimen 1-2, the oil in Specimen 2-2 is effectively recovered by CO_2 huff-and-puff. After the first cycle of CO_2 huff-and-puff, the oil recovery factor reaches 12.57%. The amount of oil produced in the small pores (<50 nm) is 19.15%, suggesting an effective recovery of saturated oil. The oil production rate of the medium pores (50–500 nm) is −46.72% because of the additional oil in the medium pores flowing from the small pores. As for large pores (>500 nm), the oil production rate is 19.57%. In the second and third cycles, CO_2 huff-and-puff maintains excellent EOR performance and delivers recovery factors of 22.40% and 37.21%, respectively, which are far higher than those for the CH_4 huff-and-puff process. Considerable increases are seen in the oil production rates of the

small pores (29.17% and 43.43%, respectively). As for medium pores (50–500 nm), the oil is effectively produced; however, the production rates are still negative (−44.39% and −26.71%, respectively) due to the remaining excess of oil, compared with the oil initially observed in the core after saturation. The oil production rates of the large pores (>500 nm) are 40.53% and 56.26%, respectively, also showing an effective recovery level. The EOR performance of CO_2 huff-and-puff is sightly degraded in the fourth cycle. The resulting recovery factor is 42.4%, and the changes in the oil production rates in the pores of different sizes are similar to those noted in the second and third cycles (47.52% for small pores, −13.31% for medium pores, and 64.27% for large pores), which are all higher than those for the last cycle. Compared with CH_4 huff-and-puff, CO_2 huff-and-puff significantly increases the oil recovery factor by 23.04%.

3.4. Comparative Analysis of EOR Effect of Different Media

With the above-stated experimental results, the oil recovery effect for shale, with different media used for the huff-and-puff process, is investigated to clarify the differences in EOR performance obtained using surfactant, CH_4, and CO_2 in the Qingshankou Formation.

During the huff-and-puff process, all media can effectively recover oil from shale in the first cycle. As the huff-and-puff process proceeds, the oil saturated in the shale gradually decreases, and the oil recovery factor grows. The EOR performance of surfactant and CH_4 is considerably degraded, but CO_2 maintains good EOR performance in the second and third cycles. Therefore, after four cycles of huff-and-puff, the ultimate oil recovery rate of CO_2 is much higher than that of surfactant or CH_4, and the ultimate oil recovery rate of CH_4 is the lowest.

The oil production in pores of different sizes is shown in Figure 11. For small pores (<50 nm), all of the three media show similar EOR performances. The oil production rates of CO_2 are slightly higher, while those of surfactant and CH_4 are close to each other. For medium pores (50–500 nm), the oil production rates are significantly different in various cores. For Core 1-1 and 1-2, the oil in the medium pores is effectively produced, and the oil production rate for CO_2 is higher than that of surfactant after multiple cycles of huff-and-puff. Meanwhile, due to the migration of some oil from the smaller pores to the larger pores during the huff-and-puff process, the ultimate oil production rates for the medium pores are negative in Core 2-1 and 2-2.

However, it should be noted that those of CO_2 are still higher than those of CH_4. In the large pores (>500 nm), the oil production is considerably differentiated for the different cores. In Core 1-1, surfactant can effectively recover oil from the large pores in the first huff-and-puff cycle. But the production rates decline in the subsequent cycles, as oil in the smaller pores flows to the larger pores, while in Core 1-2, the oil production rates in the large pores remain negative throughout the CO_2 huff-and-puff experiment, also due to oil migration from the smaller pores to the larger pores. For Core 2-1 and 2-2, both CH_4 and CO_2 can effectively recover oil in the large pores. The EOR performance of CO_2 is always higher than that of CH_4. Moreover, the excellent EOR performance of CO_2 is maintained throughout the four cycles, while CH_4 only exhibits good EOR performance in the first two cycles.

Since the experiments used drilled core samples and crude oil from the production well, there are three main limitations of this study that must be considered. Firstly, China's shale oil reservoirs are mostly formed in a continental sedimentary environment and present high heterogeneity. Although the porosity and permeability are similar between the cores, there is significant variation in pore connectivity and pore size distribution. As a result, the oil production from pores of different sizes is greatly varied for different cores during CO_2 huff-and-puff. Therefore, targeted analysis for each shale oil formation is necessary in order to clarify the actual EOR performance of the huff-and-puff process. Secondly, the shale specimens for the huff-and-puff experiments used in this paper are limited in size, and the huff-and-puff media can sweep the entire specimen. In the actual shale oil formations, the swept volume is usually limited by the permeability of the formation and the viscosity

of the injected fluid. Thus, the recovery rates obtained in experiments are usually higher than the actual recovery rates in the field. Additionally, compared with CO_2 and CH_4, the swept volume of the surfactant will be suppressed due to its poorer liquidity. Accordingly, the actual EOR performance of the surfactant may be limited. Thirdly, the experiments were carried out using produced oil. Under actual formation conditions, crude oil contains a large amount of dissolved gas, so the physical properties are different from those of the produced oil. During long-term production, the physical properties of crude oil will gradually change, which may also have an impact on the recovery rates.

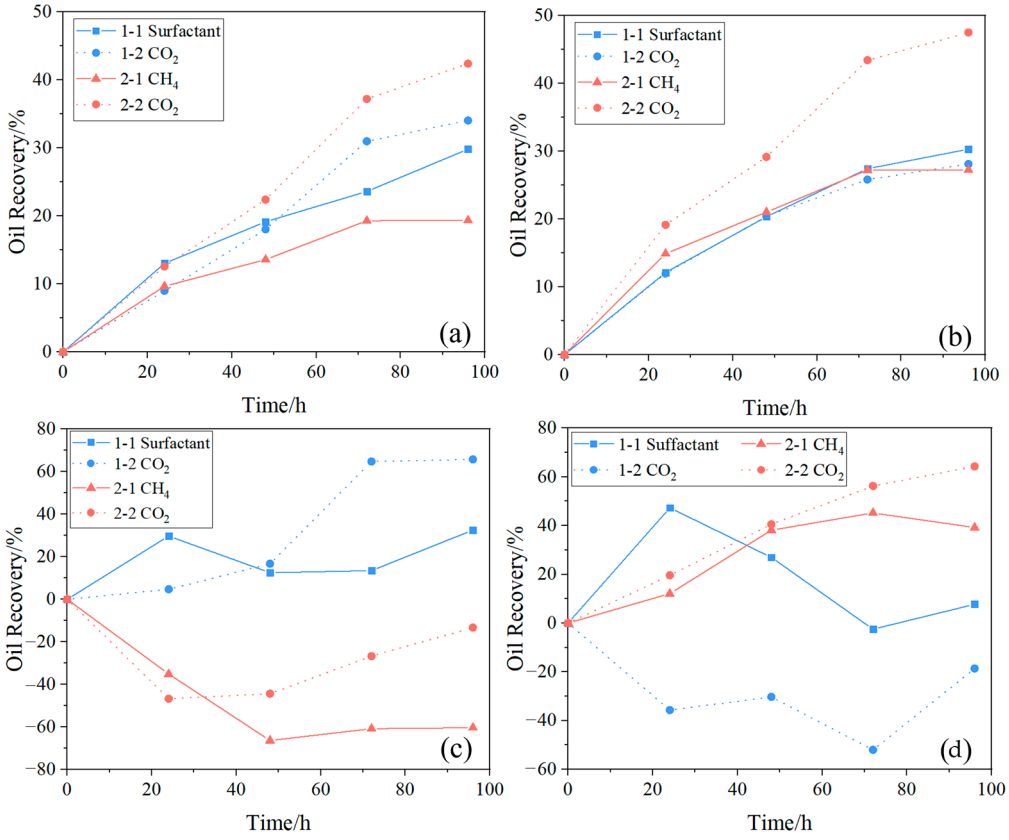

Figure 11. Comparative analysis of EOR effect during huff-and-puff of different media: (**a**) oil recovery of shale cores; (**b**) oil recovery of small pores; (**c**) oil recovery of medium pores; (**d**) oil recovery of large pores.

This study was carried out using the high clay-content shale samples in the Qingshankou Formation. In the future, the EOR performance of different media can be subsequently investigated using a wider range of shale formations with different pore structures and mineralogical compositions to clarify the most suitable EOR technology for different shale reservoirs and to provide theoretical support for the development of shale reservoirs.

4. Conclusions

The EOR performance of surfactant, CH_4, and CO_2 in a shale oil reservoir was systematically analyzed through physical simulation experiments. The conclusions are as follows: CO_2 is the most applicable medium of the three to enhance shale oil recovery in the Qingshankou Formation. It maintains good EOR performance in the second and third cycles. Therefore, after four cycles of huff-and-puff, the ultimate oil recovery of CO_2 is much higher than that of either surfactant or CH_4. Although the shale cores exhibit similar porosity and permeability, the pore connectivity is different. Thus, the oil production from pores of different sizes is greatly varied. This means that more microscopic research is necessary regarding shale reservoirs to clarify the influence of nano-pore characteristics

on EOR performance. The injection pressure of the surfactant increased the fastest, which showed a low flowability in the nano-pores. This will greatly affect the sweep efficiency in shale reservoirs. Although the EOR performance of the surfactant is significant in the core scale experiment, the actual EOR performance of the surfactant may be even lower at the field scale.

Author Contributions: Conceptualization, S.M. and H.L.; funding acquisition, S.M.; investigation, J.T., D.L. and L.L.; methodology, J.T. and S.M.; project administration, S.M.; supervision, S.M.; visualization, J.T.; writing—original draft, J.T.; writing—review and editing, S.M. All authors have read and agreed to the published version of the manuscript.

Funding: This research was funded by the "Enlisting and Leading" Science and Technology Project of Heilongjiang Province (No. RIPED-2022-JS-1740), and the Technology Project of CNPC (No. 2023ZZ08).

Data Availability Statement: The original contributions presented in the study are included in the article, further inquiries can be directed to the corresponding author.

Conflicts of Interest: Author Dongxu Li was employed by the company PetroChina Daqing Oilfield Co., Ltd. The remaining authors declare that the research was conducted in the absence of any commercial or financial relationships that could be construed as a potential conflict of interest.

References

1. Sheng, J.; Chen, K. Evaluation of the EOR potential of gas and water injection in shale oil reservoirs. *J. Unconv. Oil Gas Resour.* **2014**, *5*, 1–9. [CrossRef]
2. Song, Z.; Song, Y.; Li, Y.; Bai, B.; Song, K.; Hou, J. A critical review of CO_2 enhanced oil recovery in tight oil reservoirs of North America and China. *Fuel* **2020**, *276*, 118006. [CrossRef]
3. Fakher, S.; Imqam, A. Application of carbon dioxide injection in shale oil reservoirs for increasing oil recovery and carbon dioxide storage. *Fuel* **2020**, *265*, 116944. [CrossRef]
4. Wang, J.; Feng, L.; Steve, M.; Tang, X.; Gail, T.; Mikael, H. China's unconventional oil: A review of its resources and out-look for long-term production. *Energy* **2015**, *82*, 31–42. [CrossRef]
5. Hu, S.; Zhao, W.; Hou, L.; Yang, Z.; Zhu, R.; Wu, S.; Bai, B.; Jin, X. Development potential and technical strategy of continental shale oil in China. *Pet. Explor. Dev.* **2020**, *47*, 819–828. [CrossRef]
6. Li, G.; Zhu, R. Progress, challenges and key issues of unconventional oil and gas development of CNPC. *China Petrol. Explor.* **2020**, *25*, 1–13.
7. Tang, J.; Wang, X.; Du, X.; Ma, B.; Zhang, F. Optimization of integrated geological-engineering design of volume fracturing with fan-shaped well pattern. *Pet. Explor. Dev.* **2023**, *50*, 971–978. [CrossRef]
8. Tao, J.; Meng, S.; Li, D.; Rui, Z.; Liu, H.; Xu, J. Analysis of CO_2 effects on porosity and permeability of shale reservoirs under different water content conditions. *Geoenergy Sci. Eng.* **2023**, *226*, 211774. [CrossRef]
9. Zhou, D.; Zhang, G.; Huang, Z.; Zhao, J.; Wang, L.; Qiu, R. Changes in microstructure and mechanical properties of shales exposed to supercritical CO_2 and brine. *Int. J. Rock Mech. Min.* **2022**, *160*, 105228. [CrossRef]
10. Mojid, M.; Negash, B.; Abdulelah, H.; Jufar, S.; Adewumi, B. A state-of-art review on waterless gas shale fracturing technologies. *J. Pet. Sci. Eng.* **2021**, *196*, 108048. [CrossRef]
11. Yu, J.; Li, N.; Hui, B.; Zhao, W.; Li, Y.; Kang, J.; Hu, P.; Chen, Y. Experimental simulation of fracture propagation and extension in hydraulic fracturing: A state-of-the-art review. *Fuel* **2024**, *363*, 131021. [CrossRef]
12. Tang, J.; Zhang, M.; Guo, X.; Geng, J.; Li, Y. Investigation of creep and transport mechanisms of CO_2 fracturing within natural gas hydrates. *Energy* **2024**, *300*, 131214. [CrossRef]
13. Hu, Y.; Weijermars, R.; Zuo, L.; Yu, W. Benchmarking EUR estimates for hydraulically fractured wells with and without fracture hits using various DCA methods. *J. Pet. Sci. Eng.* **2018**, *162*, 617–632. [CrossRef]
14. Jin, L.; Hawthorne, S.; Sorensen, J.; Pekot, L.; Kurz, B.; Smith, S.; Heebink, L.; Herdegen, V.; Bosshart, N.; Torres, J.; et al. Advancing CO_2 enhanced oil recovery and storage in unconventional oil play—Experimental studies on Bakken shales. *Appl. Energy* **2017**, *208*, 171–183. [CrossRef]
15. Wu, J.; Wang, H.; Shi, Z.; Wang, Q.; Zhao, Q.; Dong, D.; Li, S.; Liu, D.; Sun, S.; Qiu, Z. Favorable lithofacies types and genesis of marine-continental transitional black shale: A case study of Permian Shanxi Formation in the eastern margin of Ordos Basin, NW China. *Pet. Explor. Dev.* **2021**, *48*, 1137–1149. [CrossRef]
16. Tian, H.; He, K.; Huangfu, Y.; Liao, F.; Wang, X.; Zhang, S. Oil content and mobility in a shale reservoir in Songliao Basin, Northeast China: Insights from combined solvent extraction and NMR methods. *Fuel* **2024**, *357*, 129678. [CrossRef]
17. Gong, D.; Bai, L.; Gao, Z.; Qin, Z.; Wang, Z.; Wei, W.; Yang, A.; Wang, R. Occurrence mechanisms of laminated-type and sandwich-type shale oil in the Fengcheng Formation of Mahu Sag, Junggar Basin. *Energy Fuels* **2023**, *37*, 13960–13975. [CrossRef]

18. Zhao, X.; Jin, F.; Liu, X.; Zhang, Z.; Cong, Z.; Li, Z.; Tang, J. Numerical study of fracture dynamics in different shale fabric facies by integrating machine learning and 3-D lattice method: A case from Cangdong Sag, Bohai Bay basin, China. *J. Pet. Sci. Eng.* **2022**, *218*, 110861. [CrossRef]
19. Dai, J.; Wang, T.; Tian, K.; Weng, J.; Li, J.; Li, G. CO_2 huff-n-puff combined with radial borehole fracturing to enhance oil recovery and store CO_2 in a shale oil reservoir. *Geoenergy Sci. Eng.* **2023**, *228*, 212012. [CrossRef]
20. Jia, B.; Tsau, J.; Barati, R. A review of the current progress of CO_2 injection EOR and carbon storage in shale oil reservoirs. *Fuel* **2019**, *236*, 404–427. [CrossRef]
21. Alvarez, J.; Saputra, I.; Schechter, D. The Impact of surfactant imbibition and adsorption for improving oil recovery in the Wolfcamp and Eagle Ford Reservoirs. *SPE J.* **2018**, *23*, 2103–2117. [CrossRef]
22. Lu, M.; Qian, Q.; Zhong, A.; Zhang, Z.; Zhang, L. Investigation on the flow behavior and mechanisms of water flooding and CO_2 immiscible/miscible flooding in shale oil reservoirs. *J. CO2 Util.* **2024**, *80*, 102660. [CrossRef]
23. Burrows, L.; Haeri, F.; Cvetic, P.; Sanguinito, S.; Shi, F.; Tapriyal, D.; Goodman, A.; Enick, R. A Literature review of CO_2, natural gas, and water-based fluids for enhanced oil recovery in unconventional reservoirs. *Energy Fuels* **2020**, *34*, 5331–5380. [CrossRef]
24. Huang, S.; Jiang, G.; Guo, C.; Feng, Q.; Yang, J.; Dong, T.; He, Y.; Yang, L. Experimental study of adsorption/desorption and enhanced recovery of shale oil and gas by zwitterionic surfactants. *Chem. Eng. J.* **2024**, *487*, 150628. [CrossRef]
25. Alvarez, J.; Saputra, I.; Schechter, D. Potential of improving oil recovery with surfactant additives to completion fluids for the Bakken. *Energy Fuels* **2017**, *31*, 5982–5994. [CrossRef]
26. Cheng, C.; Ming, G. Investigation of cyclic CO_2 huff-and-puff recovery in shale oil reservoirs using reservoir simulation and sensitivity analysis. *Fuel* **2017**, *188*, 102–111. [CrossRef]
27. Wan, T.; Zhang, J.; Jing, Z. Experimental evaluation of enhanced shale oil recovery in pore scale by CO_2 in Jimusar reservoir. *J. Pet. Sci. Eng.* **2022**, *208*, 109730. [CrossRef]
28. Li, L.; Bao, Z.; Li, L.; Li, Z.; Ban, S.; Li, Z.; Wang, T.; Li, Y.; Zheng, N.; Zhao, C.; et al. The source and preservation of lacustrine shale organic matter: Insights from the Qingshankou Formation in the Changling Sag, Southern Songliao Basin, China. *Sediment. Geol.* **2024**, *466*, 106649. [CrossRef]
29. Sun, L.; Cui, B.; Zhu, R.; Wang, R.; Feng, Z.; Li, B.; Zhang, J.; Gao, B.; Wang, Q.; Zeng, H.; et al. Shale oil enrichment evaluation and production law in Gulong Sag, Songliao Basin, NE China. *Pet. Explor. Dev.* **2023**, *50*, 505–519. [CrossRef]
30. Liu, B.; Wang, H.; Fu, X.; Bai, Y.; Bai, L.; Jia, M.; He, B. Lithofacies and depositional setting of a highly prospective lacustrine shale oil succession from the Upper Cretaceous Qingshankou Formation in the Gulong sag, northern Songliao Basin, northeast China. *AAPG Bull.* **2019**, *103*, 405–432. [CrossRef]
31. Yuan, S.; Lei, Z.; Li, J.; Mo, Z.; Li, B.; Wang, R.; Liu, Y.; Wang, Q. Key theoretical and technical issues and countermeasures for effective development of Gulong shale oil, Daqing Oilfield, NE China. *Pet. Explor. Dev.* **2023**, *50*, 562–572. [CrossRef]
32. Yang, L.; Yang, D.; Zhang, M.; Meng, S.; Wang, S.; Su, Y.; Long, X. Application of nano-scratch technology to identify continental shale mineral composition and distribution length of bedding interfacial transition zone—A case study of Cretaceous Qingshankou Formation in Gulong Depression, Songliao Basin, NE China. *Geoenergy Sci. Eng.* **2024**, *234*, 212674. [CrossRef]
33. Yang, L.; Wang, H.; Xu, H.; Guo, D.; Li, M. Experimental study on characteristics of water imbibition and ion diffusion in shale reservoirs. *Geoenergy Sci. Eng.* **2023**, *229*, 212167. [CrossRef]
34. Zhang, J.; Zhu, R.; Wu, S.; Jiang, X.; Liu, C.; Cai, Y.; Zhang, S.; Zhang, T. Microscopic oil occurrence in high-maturity lacustrine shales: Qingshankou Formation, Gulong Sag, Songliao Basin. *Pet. Sci.* **2023**, *20*, 2726–2746. [CrossRef]
35. Wang, X.; Cui, B.; Feng, Z.; Shao, H.; Huo, L.; Zhang, B.; Gao, B.; Zeng, H. In-situ hydrocarbon formation and accumulation mechanisms of micro- and nano- scale pore-fracture in Gulong shale, Songliao Basin, NE China. *Pet. Explor. Dev.* **2023**, *50*, 1105–1115. [CrossRef]